Detection method for the degree of damage to Korla fragrant pears based on electrical properties

Yang Liu[1,3], Yifan Xia[1,3], Jikai Che[1,3], Haipeng Lan[1,3], Hong Zhang[1,2*]

(1. *Modern Agricultural Engineering Key Laboratory at Universities of Education Department of Xinjiang Uygur Autonomous Region, Tarim University, Alaer 843300, Xinjiang, China*;
2. *College of Water Resources and Architectural Engineering, Tarim University, Alaer, Xinjiang 843300, China*;
3. *College of Mechanical and Electrical Engineering, Tarim University, Alaer, Xinjiang 843300, China*)

Abstract: To solve challenges in the automated and rapid, non-destructive detection of damage to Korla fragrant pears, this study explored the laws influencing the impact of load on damage to fragrant pears during ripening. A comparative analysis of the external features and microscopic structural changes before and after fragrant pear damage was performed. The electrical parameters of fragrant pears were collected using the fruit electrical parameter detection system, including parallel equivalent capacitance (*Cp*), parallel equivalent resistance (*Rp*), and complex impedance (*Z*). The correlations between the electrical parameters of fragrant pears and the degree of damage were analyzed. A detection model for the degree of damage to Korla fragrant pears was constructed using partial least squares regression (PLSR), support vector regression (SVR), and particle swarm optimization-least squares support vector regression (PSO-LSSVR), and the optimal model was determined and screened. The results showed that, in the same ripening, the damaged area of fragrant pears increased as the falling height increased. Given equal impact loads, the damage area of fragrant pears increased as the picking time increased. *Cp*, *Rp*, and *Z* were strongly correlated with the damaged area of fragrant pears. When the test frequency was 1 kHz, the PSO-LSSVR model showed the optimal detection performance (R^2 = 0.9172, RMSE = 117.56) for the damaged area of fragrant pears. These research results provide a theoretical reference for the quality assessment and storage regulation of fragrant pears.

Keywords: Korla fragrant pear, electrical properties, degree of damage, non-destructive detection
DOI: 10.25165/j.ijabe.20251803.8927

Citation: Liu Y, Xia Y F, Che J K, Lan H P, Zhang H. Detection method for the degree of damage to Korla fragrant pears based on electrical properties. Int J Agric & Biol Eng, 2025; 18(3): 215–222.

1 Introduction

The Korla fragrant pear has a thin pericarp, crisp pulp, rich juice, sweet taste, and plentiful nutrients. It has extremely strong growth regions and is known as the"treasure of pears"The Korla fragrant pear is mainly produced in Korla and Aksu in Xinjiang, China, as it is a protected product in the national geographical region[1-3]. The Korla fragrant pear suffers mechanical damage during harvesting, grading, packaging, transportation, storage, and other processing stages[4]. Damaged fragrant pears are discarded directly before storage. Annually, more than 38% of fragrant pear waste is caused by different types of mechanical damage, which seriously restricts the development of the fragrant pear industry[5]. According to industrial standards and relevant studies, fragrant pears with some surface defects or damage still have some marketing value[6,7]. Fragrant pears with different degrees of damage can be used in different processing channels or stored and sold at different times. Therefore, the development of a non-destructive detection method to determine the degree of damage of fragrant pears is urgently needed to enable the suitable use of damaged fragrant pears, thereby decreasing the waste, increasing the utilization, and extending the industrial processing chain of fragrant pears.

Fruit damage is usually divided into explicit damage and implicit damage[8]. Explicit damage to fruit can be observed by the naked eye through the brightness, wrinkles, and external pericarp features, enabling fruit with explicit damage to be distinguished from normal fruit. The explicit damage of fruit is mainly recognized by the geometric size of tissue browning. The damage area method, damage volume method, and damage depth method are generally used to measure and detect explicit damage to fruit. In these, the damaged fruit is stored at room temperature for more than 24 h to ensure full browning of the damaged position. The area, volume, or depth of browning are measured to represent the degree of damage[9]. However, this measurement method is time-consuming, which is disadvantageous for the rapid detection of the degree of damage to fruit. With implicit damage, the fruit cell tissues are more integral and the oxidation rate of enzymatic substances in fruits is relatively low compared to explicit damage[10]. It is very difficult to observe and distinguish this damage by the naked eye from external information and pericarp features. Due to its limitations in the quantitative evaluation of fragrant pear damage, the replacement of artificial identification by a reasonable non-destructive detection technology would enable the non-destructive detection of the degree of damage of fragrant pears before storage, which would enable the optimal processing mode to be selected after harvesting. Such a

Received date: 2024-03-14 **Accepted date:** 2025-04-07
Biographies: Yang Liu, PhD, Associate Professor, research interest: agricultural products processing technology, Email: 120150012@taru.edu.cn; **Yifan Xia**, postgraduate student, research interest: agricultural products processing technology, Email: 2435345995@qq.com; **Jikai Che**, Postgraduate Student, research interest: agricultural products processing technology, Email: 3115261705@qq.com; **Haipeng Lan**, PhD, Professor, research interest: agricultural products processing technology, Email: lanhaipeng@126.com.
***Corresponding author: Hong Zhang**, MS, Lecturer, research interest: agriculture geographic information system. College of Water Resources and Architectural Engineering, Tarim University, Alaer 843300, Xinjiang, China. Tel: +86-18845161657, Email: 120230116@taru.edu.cn.

method would provide theoretical guidance for quality grading and storage technology regulation.

Non-destructive detection technologies are reasonably mature. With characteristics of non-destructive detection, simple operation, high convenience, and high sensitivity, electrical analytical technologies have been widely applied in the identification of fruit damage and quality[11,12]. Korla fragrant pears have a thin pericarp, juicy pulp, and contain many charged particles. After the pears are damaged, changes to their internal substances and energy occur, which in turn influences the distribution and strength of the bioelectric field[13]. This is macroscopically manifested as changes in the electrical properties. These phenomena lay a good foundation for the detection of damage to fragrant pears based on their electrical properties via an approach that is rapid, sensitive, and straightforward. Jiang et al.[14-16] studied trends in the electrical parameters of fruit after damage and found obvious differences between undamaged and damaged fruit. Thus, there has been some exploration of the relationship between electrical parameters and fruit damage. An et al.[17] identified internal damage to fragrant pears based on electrical feature detection technology, but a detection model of the degree of internal damage was not developed. Bian et al.[18] predicted the browning area of apples after injury based on dielectric properties, but failed to predict the degree of damage to the apples. Fan et al.[19] detected static pressure damage to Korla fragrant pears at three picking times by using the technological mean based on electrical properties. They built a mathematical model to describe the relationship between the electrical parameters of these three crops of fragrant pear and the damaged area. This mathematical model conformed to a quadratic equation with one unknown variable. However, since this model was based on electrical parameter variations before and after fragrant pear damage, it was not applicable to online detection but only to predict damage to fragrant pears from the same maturity. Based on the above literature review, curve fitting was performed for the electrical parameters and degree of damage, but this was not applicable to the detection of damage to all fruit. Therefore, there is an urgent need for a method with a stable modeling effect to enable the rapid and non-destructive evaluation of fragrant pears.

As important artificial intelligence algorithms, machine-learning methods are developing rapidly. Recently, machine-learning methods like partial least squares regression (PLSR), support vector regression (SVR), and particle swarm optimization-least squares support vector regression (PSO-LSSVR) have been extensively applied to predict the static pressure damage of fragrant pears, the soluble solid content of apples, and the price of agricultural products due to their quick training and high prediction accuracy[20-22]. However, there has been little research combining electrical properties and machine-learning methods for the detection of fruit damage based on PLSR, SVR, and PSO-LSSVR.

In this study, the influence of impact loads on the damage to fragrant pears was explored. The external features and microstructural changes of the damaged fragrant pears were analyzed. Electrical parameters of the damaged fragrant pears were collected using the electrical parameter detection system for fruit, and their correlations with the degree of damage were determined. The electrical parameters were used as the system inputs, and the damage area was used as the system output. On this basis, some detection models of the degree of damage to Korla fragrant pear were built using PLSR, SVR, and PSO-LSSVR. The optimal detection model was determined and screened to ultimately achieve the effective prediction of the degree of damage to fragrant pears.

2 Materials and methods

2.1 Test materials

Korla fragrant pear samples: High-quality fragrant pears from Southern Xinjiang, China were collected from the Shituan Conventional Management Pear Garden in Alaer City. The trees were 12 years old. Samples were collected every four days from September 1-29, 2019, resulting in eight sampling times. The average weight of the chosen fragrant pears was 125±3 g. For each sampling, 70 fragrant pears were collected, resulting in a total of 560 fragrant pear samples. These were carried to the laboratory immediately after picking for the impact damage test. The experiment required the selection of Korla fragrant pears of similar shape and size, without distortion, implicit damage, disease or insect damage, and with uniform color at the same picking time.

2.2 Impact damage test

The impact damage test for fragrant pears in different ripening periods was implemented using a self-made impact damage testbed. Corrugated boards were paved on the testbed, onto which the fragrant pears fell. The testbed was divided into the hoisting gear and adsorption device (Figure 1). The adsorption device comprised a vacuum generator, a sucker, and an air compressor. The hoisting gear consisted of a lead screw, a linear guideway, a pneumatic motor, and an extending arm. The operational steps were as follows. The sucker was lifted to the appointed height by the hoisting gear, and a sample was adsorbed onto the sucker through the adsorption device. The suction was turned off, causing the fragrant pear to fall onto the contact material of the platform surface, resulting in impact damage on the testbed. First, the falling height was adjusted. Fragrant pears were damaged when the falling height was 30 cm. The pericarp of the fragrant pear broke and juice leaked out when the falling height was 150 cm. At this point, the falling test was terminated. Finally, the falling height was set to 30, 50, 70, 90, 110, 130, and 150 cm. Ten repetitions were performed in each group of tests. The electrical parameters of each fragrant pear were measured immediately after the impact damage test. Finally, the degree of damage was measured. Test data were recorded and the mean values were calculated. The surface damage area of fragrant pears could be recognized by the naked eye, which was conducive to judging damage degrees. This also was used as a major index to evaluate apparent quality of fruits[5]. Hence, the degree of damage of fragrant pears was determined from the damage area.

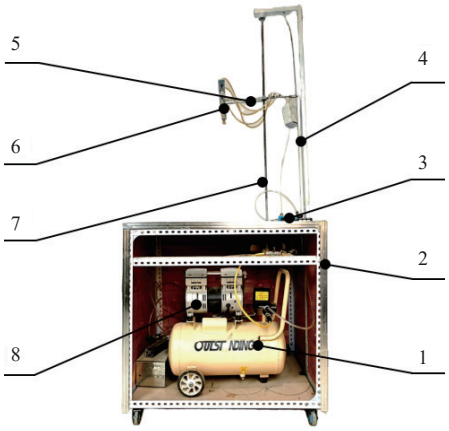

1. Air compressor; 2. Engine body; 3. Vacuum generator; 4. Linear guideway; 5. Cantilever arm; 6. Sucker; 7. Leading screw; 8. Pneumatic motor

Figure 1 Self-made testbed for impact damage

After the Korla fragrant pears were damaged, they were kept at room temperature to allow them to fully brown. The pericarp at the damaged position was removed using a knife. The major semi-axis (a) and the minor semi-axis (b) of the damaged area were measured (Figure 2). The damaged area was calculated using the measurement method proposed by Zhang[23] and Komarnicki[24] [Equation (1)].

$$S = \pi ab \tag{1}$$

where, S is damaged area of fragrant pears, mm^2; a is major semi-axis of the oval damaged area, mm; b is minor semi-axis of the oval damaged area, mm.

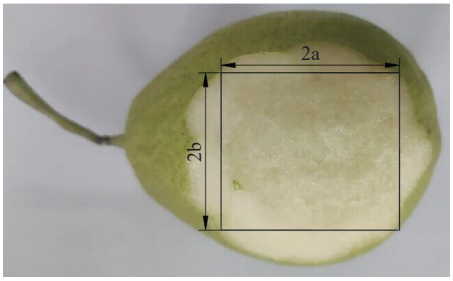

Figure 2 Measurement diagram of damaged area of fragrant pears

2.3 Measurement test of electrical parameters of fragrant pears

Electrical parameters of fragrant pears were collected using a self-made electrical property detection system (Figure 3). The LCR test bridge was preheated for 1 h before use. Subsequently, a zeroing operation was performed to decrease errors. After preheating, the shielded box was opened. The lifting and falling of the upper parallel electrode plate were controlled by a motor for the rough adjustment of their distance so the two electrode plates were in contact with the fragrant pear. Next, the fine adjustment of the upper parallel electrode plate was performed by rotating the hand wheel to ensure that the electrodes were in contact with two relative vertical points on the surface equator regions of the fragrant pear. The orientation of the fragrant pear in the shielded box was kept consistent. The conductive sponge was pasted onto the electrode surface, and the air space was eliminated after contact with the fragrant pear. At this moment, the fragrant pear sample was clamped into copper electrode plates (diameter: 30 mm) with a fixed pre-tightening force of 0.7 N, and the shielded box was closed. The electrode plates were connected to the external mechanical structure by insulating bars. They were put in the shielded case with the fragrant pear to measure the electrical parameters and prevent errors caused by external magnetic disturbances. The electrical parameters of each fragrant pear were measured under a test voltage of 1 V and different test frequencies (1 MHz, 100 kHz, 10 kHz, 1 kHz, and 100 Hz). Parallel equivalent capacity (Cp), parallel equivalent resistance (Rp), and complex impedance (Z) are relatively sensitive to fruit damage and are often used to evaluate the degree of damage to fruit[25]. In this study, Cp, Rp, and Z were chosen as major electrical parameters for damaged fragrant pears. Cp reflects the charge storage capacity at a given potential difference. Generally, charges move in an electric field due to the influences of stresses. The presence of media between conductors hinders the movement of charges, resulting in their accumulation on the conductor. As a result, the charges are accumulated and stored[26]. Rp is relative to alternating signals at a certain frequency. In an alternating electric field, resistance, capacitance, and inductance may hinder the flow of current. Hence, Rp is the vector sum of resistance, capacitive resistance, and inductive reactance[27]. Z reflects the hindering effects of resistance, inductance, and capacitance against a current. It refers to the sum of resistance and inductance in the biological equivalent composite circuit composed of resistance, capacitance, and inductance[28].

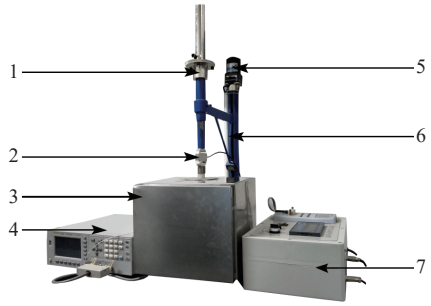

Note: 1. Fine adjustment hand wheel; 2. Force sensor; 3. Shielded box; 4. Test bridge; 5. Loading motor; 6. Support; 7. Force controller

Figure 3 Electrical properties detection system

2.4 Scanning electron microscopy

2.4.1 Sample preparation

One damaged position of each fragrant pear was chosen as the sample collection position. The pericarp was removed using a scalpel, and a cubic sample of subcutaneous pulp tissue (1×1×1 cm^3) was collected and placed in glutaraldehyde solution. The samples were put in a refrigerator (4°C) for 24 h before follow-up testing.

2.4.2 Gradient dehydration:

(1) 30% ethyl alcohol: fragrant pear samples were immersed for 40 min.

(2) 50% ethyl alcohol: fragrant pear samples were immersed for 40 min.

(3) 70% ethyl alcohol: fragrant pear samples were immersed for 40 min.

(4) 90% ethyl alcohol: fragrant pear samples were immersed for 40 min.

(5) 95% ethyl alcohol: fragrant pear samples were immersed for 40 min.

(6) 100% ethyl alcohol: fragrant pear samples were immersed for 40 min.

(7) 100% ethyl alcohol: fragrant pear samples were immersed for 40 min.

(8) 100% ethyl alcohol: 100% acetone (1:1): fragrant pear samples were immersed for 40 min.

(9) 100% acetone: fragrant pear samples were immersed for 40 min.

(10) 100% acetone: fragrant pear samples were immersed for 40 min.

2.4.3 CO_2 replacement of acetone

The chosen fragrant pear samples were dried using a critical point dryer.

2.4.4 Metal spraying

The dried fragrant pear samples were coated with a consistent thickness of film using an ion sputter coater.

2.4.5 Scanning electron microscopy

Scanning electron microscopy (SEM) was used to observe and capture images of the tissue structures of the fragrant pear samples.

2.5 Modeling method

This study used three modeling methods: PLSR, SVR, and PSO-LSSVR. Detection models for the damage area to fragrant pears during ripening periods were constructed. The model inputs were

Cp, *Rp*, and *Z*. The model outputs were the damaged areas of fragrant pears.

2.5.1 PLSR model

PLSR is the most extensively used linear modeling technique. It integrates the advantages of typical correlation analysis, multi-variant linear regression analysis, and principal component analysis (PCA)[29]. Given the unified algorithm framework, PLSR results in a comprehensive factor with the strongest interpretation capacity for dependent variables through information decomposition. It also eliminates relevant disturbance factors, thereby producing regression results with strong robustness and high accuracy. PLSR modeling allows the sample size to be smaller than the variable quantity. It has a very good identification ability for eigenvectors and effectively eliminates multiple correlations. The PLSR model can provide a good summary of dependent variable information.

2.5.2 SVR model

SVR is an application branch of support vector machine (SVM) in the regression field. SVM is mainly used to solve pattern recognition problems, while SVR is applied for data fitting[30]. Similar to the SVM classification model, SVR is a non-probabilistic algorithm. It maps data onto a high-dimensional space by using the kernel function. The maximum interval between the optimal hyper-plane and the training data is searched in this high-dimensional space, producing the regression model. Different from traditional regression models, SVR transforms the regression problem into a function that approaches the real function. In practical applications, the model can be adjusted by using different kernel functions and hyper-parameters to improve the fitting effect. SVR can process non-linear problems. With high-dimensional data processing capacity and outstanding generalization ability, it has robustness to outliers. Hence, the SVR model achieves a high prediction accuracy.

2.5.3 PSO-LSSVR model

The least squares support vector regression (LSSVR) algorithm is the least squares support vector machine for regression prediction. Scholars have applied the LSSVR algorithm to non-linear prediction modeling and achieved the thinning of solutions to the LSSVR algorithm by using pruning technology. The main idea of LSSVR is to map data non-linearity into a high-dimensional feature space through the mapping function and then solve the regression problem in the high-dimensional feature space.

Particle swarm optimization (PSO) is a global random searching algorithm based on swarm intelligence that simulates the migration and bunching behaviors of bird flocks during hunting[31]. The PSO algorithm searches for the optimal solution from candidate solutions through a global searching strategy and displacement velocity mode of particles, obtaining the optimal solution of particle and particle swarm by updating the particle state continuously. This algorithm has a strong searching ability and it is easy to execute, requiring minimal parameter adjustments. For LSSVR parameter optimization, the parameter space full searching method is usually used, so it is very difficult to determine a reasonable parameter range. PSO can generate swarm intelligence through the cooperation and competition of particles to guide optimal searching[32]. The principle is simple. Additionally, PSO requires few parameters and has a high convergence speed. Its global searching ability can effectively offset difficulties in LSSVR parameter optimization. Therefore, PSO and LSSVR were combined in this study to increase the learning and generalization abilities of the model, increasing its prediction accuracy.

2.5.4 Determination of the optimal prediction model

To select the optimal prediction model, the prediction performance of the models was evaluated according to their root-mean-square error (RMSE) and coefficient of determination of the linear regression line (R^2). Generally, a high-accuracy model has a low RMSE and high R^2. RMSE and R^2 were calculated according to Equations (2)-(3).

$$\mathrm{RMSE} = \sqrt{\frac{\sum_{i=1}^{N}\left(M_j - T_j\right)^2}{N}} \tag{2}$$

$$R^2 = 1 - \frac{\sum_{i=1}^{N}(M_j - T_j)^2}{\sum_{i=1}^{N}(M_j - \overline{T}_j)^2} \tag{3}$$

where, M_j and T_j are the measured values and prediction values of data j, respectively; $\overline{T}_j$ is the mean of the measured values; N is the total number of data.

3 Results and analysis

3.1 Effects of impact load on fragrant pear damage

The variation in the damaged area of fragrant pears with different falling heights in different ripening periods is shown in Figure 4. Given the same ripening, the damaged area of fragrant pears increased as the falling height increased. Given the same falling height, the damaged area of fragrant pears increased as the ripening increased. A greater falling height increased the impact speed and impact energy of the fragrant pears, resulting in a larger damage area[5]. At the beginning and end of fragrant pear ripening, there was a relatively close relationship between falling height and damaged area. In the middle of ripening, the relationship between the falling height and the damaged area was not close. When the falling height was 30 cm, the fragrant pears in the ripening period of September 1–17 were not damaged. However, fragrant pears picked after September 21 were damaged, which could not be recognized by the naked eye. When the falling height was less than 110 cm, the fragrant pear pericarp was not damaged yet. When the falling height was 130 cm, the pericarp of fragrant pears from September 1–13 was not damaged, but the pericarp of fragrant pears from September 17–29 began to be damaged. When the falling height was 150 cm, the pericarp of fragrant pears from all ripening periods was damaged: fruits were fully cracked, accompanied by collapsed pulp and the leakage of juice (Figure 5).

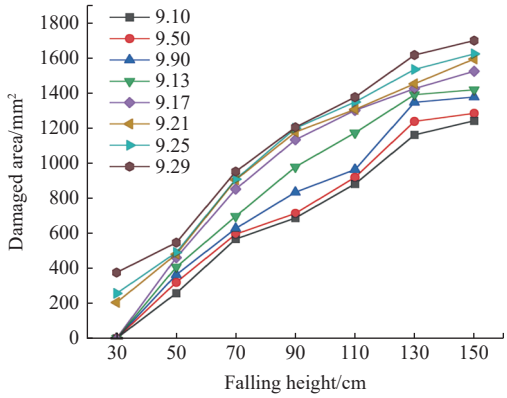

Figure 4 Relationship between falling height and damage area of fragrant pears during different ripening periods

3.2 Microstructure of damaged fragrant pears

To reveal the mechanism of mechanical damage to fragrant

Figure 5 External characteristics of damage on fragrant pear skin when falling height was 150 cm

pears, the microstructure at the damaged positions was observed by SEM and compared with that of undamaged fragrant pears. The microstructure of pulp tissues of the damaged fragrant pears picked on September 1, when the falling height was 30, 50, and 70 cm, is shown in Figure 6. Figure 6a shows that the pulp tissue cell spaces and cell walls of undamaged fragrant pears were complete, compact, and had consistent structures, with cells in a networked regular arrangement. The circles are cell spaces, which were relatively complete. The fragrant pears developed a small degree of damage when they fell from a height of 30 cm. This is known as implicit damage, manifested by mild cell damage to pulp tissues and local collapse (Figure 6b). As the load increased, there was large-scale cell damage, resulting in hardly any complete cell structures (Figure 6c). When the falling height increased to 70 cm, the pronounced collapse and folding of whole cell tissues occurred, accompanied by the disappearance of cell spaces (Figure 6d). As the load increased, the degree of damage increased and the microstructure of the fragrant pear pulp was more seriously damaged. The degree of damage of fragrant pear was proportional to the collapse and folding of the cell microstructure. This is consistent with the research conclusions of Li et al[33]. The fragrant pear fruit is rich in water and ionic compounds[34]. Combining the external features and microstructural damage of damaged fragrant pears, it was found that the cell structure was damaged after the fragrant pears were impacted, accompanied by the large-scale leakage of juice that was rich in water and electrolytes. As the degree of damage increased, the cell damage was more serious and more water and electrolyte leakage occurred[4]. Therefore, the macroscopic electrical properties of fragrant pears with different degrees of damage may differ.

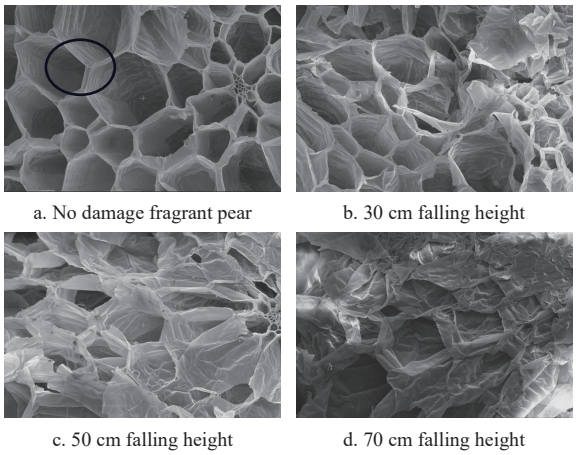

a. No damage fragrant pear b. 30 cm falling height

c. 50 cm falling height d. 70 cm falling height

Note: Scale 100 μm

Figure 6 Microstructure of fleshy tissue of damaged fragrant pear under different falling height

3.3 Correlation analysis between electrical parameters and damage area to fragrant pears

The correlation between the electrical parameters and the damage area was determined using the Pearson correlation analysis method. Figure 7 shows that, under five test frequencies, *Cp* was proportional to the damage area, while *Rp* and *Z* were negatively correlated to the damage area. *Rp* showed the strongest correlation with the damage area. These results confirmed the strong correlations between the electrical parameters and damage area to fragrant pears and the potential for the detection of the damage area to fragrant pears based on a machine-learning method.

3.4 Construction of a damage area detection model for fragrant pears based on electrical parameters and machine-learning methods

3.4.1 Detection of damage area in fragrant pear based on PLSR

Cp, *Z*, and *Rp* were used as the system inputs, and the damage area was used as the output. Among 56 datasets, 70% were chosen as the training set to train the model, while the other 30% were chosen as the test set and input into the trained prediction model to obtain the prediction results. A linear fitting was performed on the prediction results and measurement values (Table 1). R^2 differed among the test sets of the PLSR prediction model under different test frequencies. When the test frequency was 1 MHz, 10 kHz, 100 kHz, and 100 Hz, the R^2 values for the test set were lower than 0.8, indicating that the PLSR model had a poor prediction effect. When the test frequency was 1 kHz, the detection model had a good prediction effect, with R^2 = 0.8094 and RMSE = 200.49. Therefore, when the test frequency was 1 kHz, it was feasible to detect the damage area to fragrant pears by combining electrical parameters and the PLSR model.

Table 1 Damage area prediction results based on PLSR model

Frequency	Training set		Test set	
	R^2	RMSE	R^2	RMSE
1 MHz	0.7360	240.40	0.1958	411.82
100 KHz	0.8108	203.53	0.6068	287.97
10 KHz	0.9145	136.38	0.7196	243.18
1 KHz	0.8799	162.15	0.8094	200.49
100 Hz	0.8196	198.71	0.7942	208.35

3.4.2 Detection of damage area in fragrant pear based on SVR

Cp, *Z*, and *Rp* were used as the system inputs, and the damage area was used as the output. Among 56 groups in the dataset, 70% were chosen as the training set to train the model, and the other 30% were chosen as the test set and input into the trained prediction model to obtain the prediction results. A linear fitting was performed for the prediction results and measurement values (Table 2). R^2 differed among the SVR prediction model test sets under different test frequencies. When the test frequency was 100 kHz, R^2 was 0.7969 (<0.8), indicating a poor prediction effect.

Table 2 Damage area prediction results based on SVR model

Frequency	Training set		Test set	
	R^2	RMSE	R^2	RMSE
1MHz	0.8282	195.40	0.8765	353.29
100KHz	0.8296	208.34	0.7969	209.04
10KHz	0.9465	114.45	0.9258	149.45
1KHz	0.9472	118.81	0.8628	149.13
100Hz	0.8953	166.56	0.8338	224.08

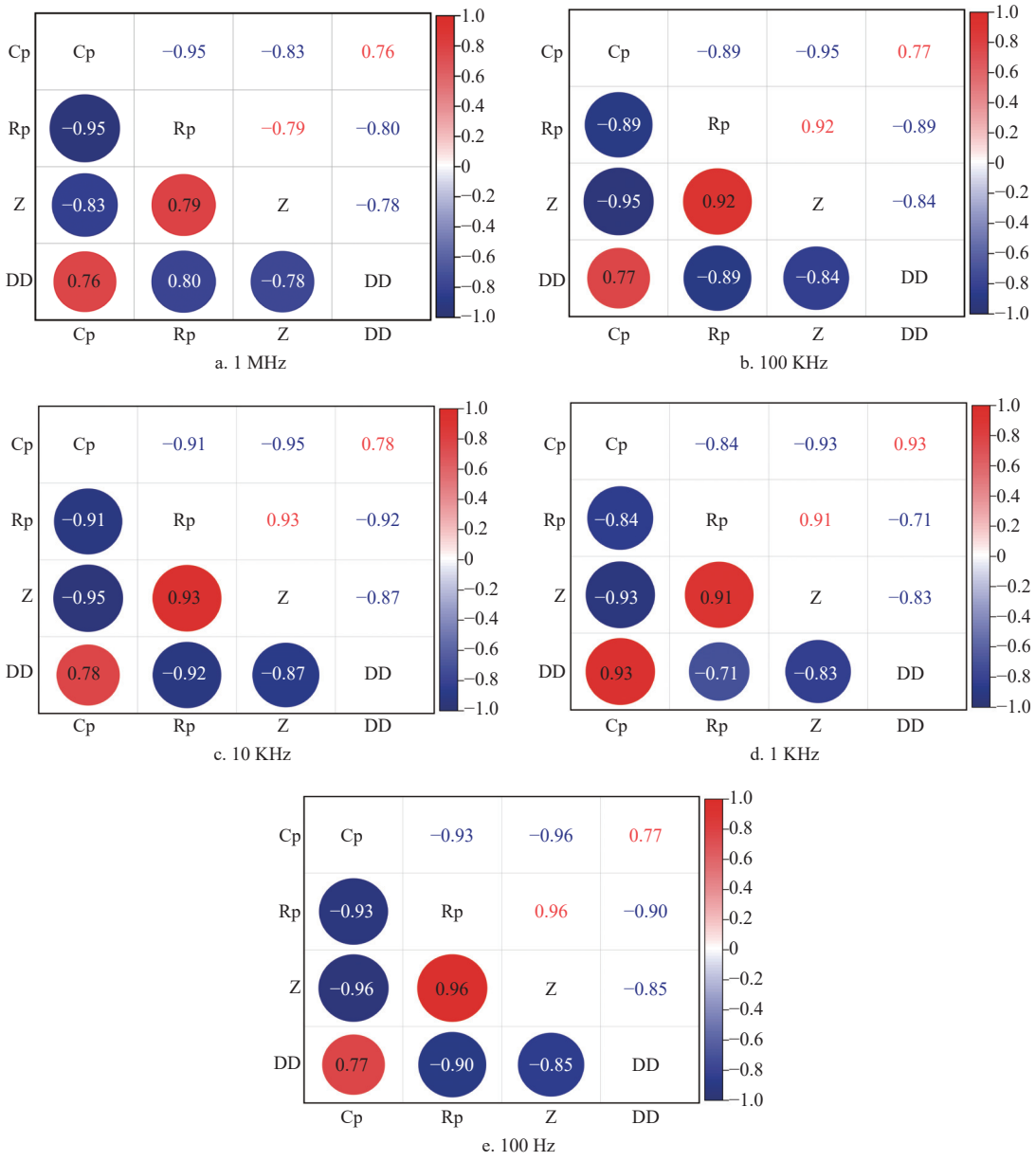

Note: DD represents damage area.

Figure 7 Correlation between electrical parameters and damage area to fragrant pears

When the test frequency was 1 MHz, 10 kHz, 1 kHz, and 100 Hz, R^2 was greater than 0.8, indicating the good prediction effect of the SVR model. The best prediction effect was when the test frequency was 10 kHz, with R^2 = 0.9258 and RMSE = 149.45. By combining electrical parameters and the SVR method, the detection of the damage area to the fragrant pears was optimal, with this approach showing some feasibility.

3.4.3 Detection of damage area in fragrant pear based on PSO-LSSVR

Cp, *Z*, and *Rp* were used as the system inputs, and the damage area was used as the output. Of 56 groups in the dataset, 70% were chosen as the training set to train the model, while the other 30% were chosen as the test set and input into the trained prediction model to obtain the prediction results. A linear fitting was performed on the prediction results and measurement values (Table 3). The PSO-LSSVR detection model showed the optimal prediction effect under different test frequencies, and the R^2 (>0.86) differed slightly among test sets. This revealed that the PSO-LSSVR model could predict the damage area to fragrant pears well. When the test frequency was 1 MHz, the R^2 of the test model peaked, but the RMSE was relatively large (300.74). When the test frequency was 1 kHz, R^2 was 0.9172, and the goodness of fit of the model was relatively high. Additionally, the RMSE of the test model was relatively small (117.56). The PSO-LSSVR model of the damage area to fragrant pears was compared comprehensively under different test frequencies, revealing the best prediction effect when the test frequency was 1 kHz. Therefore, the PSO-LSSVR method in combination with electrical parameters could detect the damage area to fragrant pears well.

Table 3 Damage area prediction results based on PSO-LSSVR model

Frequency	Training set		Test set	
	R^2	RMSE	R^2	RMSE
1MHz	0.8680	171.78	0.9293	320.74
100KHz	0.8738	179.29	0.8805	161.88
10KHz	0.9792	72.35	0.9077	137.92
1KHz	0.9692	90.94	0.9172	117.56
100Hz	0.8291	216.37	0.8634	189.63

3.5 Selection of the optimal prediction model

To select the optimal detection model, the R^2 and RMSE values of the PLSR model, SVR model, and PSO-LSSVR model were compared. It was found that the trained PLSR, SVR, and PSO-LSSVR models could predict the damage area to fragrant pears by acquiring *Cp*, *Z*, and *Rp*. Under different electrical test frequencies, the PLSR model showed a poorer prediction ability than the SVR and PSO-LSSVR models. When the test frequency was 10 kHz, R^2 = 0.9258 and RMSE = 149.45 for the SVR model. When the test frequency was 1 kHz, R^2 = 0.9172 and RMSE = 117.56 for the PSO-LSSVR model. The prediction performance of the SVR and PSO-LSSVR models was comprehensively compared. It was found that R^2 differed slightly among test sets, but the RMSE of the PSO-LSSVR model was far smaller than that of the SVR model. Overall, the PSO-LSSVR model at a test frequency of 1 kHz achieved the optimal prediction accuracy for the damage area to fragrant pears (R^2 = 0.9172 and RMSE = 117.56).

4 Conclusions

Given the same impact load, the damage area to fragrant pears increased as the ripening period increased. Given the same ripening time, the damage area to fragrant pears increased as the impact load increased and the damage to the pulp microstructure was more serious. The degree of damage to fragrant pears was proportional to the collapse and folding of the cell microstructure. *Cp*, *Rp*, and *Z* were strongly correlated with the damage area to fragrant pears, with *Rp* showing the strongest correlation. A comparison of the prediction performance of the PLSR, SVR, and PSO-LSSVR models revealed that all three trained models could detect the damage area to fragrant pears under different test frequencies. PSO-LSSVR was the optimal model for detecting the damage area to fragrant pears by combining electrical properties and machine-learning methods when the test frequency was 1 kHz (R^2 = 0.9172 and RMSE = 117.56). These research results provide theoretical guidance for quality grading and technological storage regulation for fragrant pears.

Acknowledgements

We acknowledge that this work was financially supported by the Chinese Natural Science Foundation (Grants No. 32202139 and 32260618), the Tarim University President Fund Project (Grant No. TDZKSS202427), and the Bingtuan Guiding Science and Technology Plan Program (Grant No. 2022ZD094).

[References]

[1] Xia Y F, Liu Y, Zhang H, Che J K, Liang Q. Study on color detection of Korla fragrant pears by near-infrared spectroscopy combined with PLSR. Horticulturae, 2025; 11: 352.

[2] Liu Y, Tang Y R, Zhang H, Niu H, Lan H P. Model for estimating the weight-loss ratio of damaged Korla fragrant pears. Int J Agric & Biol Eng, 2024; 17(1): 261–266.

[3] Che J K, Liang Q, Xia Y F, Liu Y, Li H S, Hu N G, et al. The study on nondestructive detection methods for internal quality of Korla fragrant pears based on near-infrared spectroscopy and machine learning. Foods, 2024; 13: 3522.

[4] Liu Y, Niu X Y, Tang Y, Li S Y, Lan H P, Niu H. Internal quality prediction method of damaged Korla fragrant pears during storage. Horticulturae, 2023; 9: 666.

[5] Wu J. Study on dynamic viscoelastic property and impact bruise of Korla pear. PhD thesis, Northwest A&F University, Yangling, Shanxi, China, 2011. (in Chinese)

[6] Yu S H, Lan H P, Li X L, Zhang H, Zeng Y, Niu H, et al. Prediction method of shelf life of damaged Korla fragrant pears. Journal of Food Process Engineering, 2021; 44(13): e13902.

[7] NY/T 585-2002. Agricultural Industry Standard. Ministry of Agriculture of the PRC: Beijing, China, 2002; p. 3. (in Chinese)

[8] Hounhouigan M H, Linnemann A R, Ingenbleek P T M, Soumanou M M, van Trijp H C M, van Boekel M A J S. Effect of physical damage and storage of pineapple fruits on their suitability for juice production. Journal of Food Quality, 2014; 37(4): 268–273.

[9] Umezuruike L O, Pankaj B P. Bruise damage measurement and analysis of fresh horticultural produce—A review. Postharvest Biology and Technology, 2014; 91: 9–24.

[10] Yousefi S, Farsi H, Kheiralipour K. Drop test of pear fruit: Experimental measurement and finite element modelling. Biosystems Engineering, 2016; 147: 17–25.

[11] Acácio F N, Nelson C O, Erlon R C, Helinando P O. Determination of mango ripening degree by electrical impedance spectroscopy. Computers and Electronics in Agriculture, 2017; 143: 222–226.

[12] Guo W C, Fang L J, Liu D Y, Wang Z W. Determination of soluble solids content and firmness of pears during ripening by using dielectric spectroscopy. Computers and Electronics in Agriculture, 2015; 117; 226–233.

[13] Jha S N, Narsaiah K, Basediya A L, Sharma R, Jaiswal P, Kumar R, et al. Measurement techniques and application of electrical properties for nondestructive quality evaluation of foods—A review. Journal of Food Science and Technology, 2011; 48; 387–411.

[14] Jiang Y, Shiina T, Nakamura N, Nakahara A. Electrical conductivity evaluation of postharvest strawberry damage. Journal of Food Science, 2001; 66(9): 1392–1395.

[15] Sun H, Wan F, Huang Y, Xu Z, Huang X. Evaluation of a new method to assess blueberry bruising based on intracellular and extracellular water ratios. Scientia Horticulturae, 2024; 328: 112896.

[16] Matsumoto S, Sugino N, Watanabe T, Kitazawa H. Bioelectrochemical impedance analysis and the correlation with mechanical properties for evaluating bruise tolerance differences to drop shock in strawberry cultivars. European Food Research and Technology, 2022; 248(3): 807–813.

[17] An J, Luo X Z, Xiong L J, Tang X Y, Lan H P. Discrimination of inner injury of Korla fragrant pear based on multi-electrical parameters. Foods, 2023; 12: 1805.

[18] Bian H X, Shi P, Tu P. Determination of physicochemical quality of bruised apple using dielectric properties. Journal of Food Measurement and Characterization, 2020; 14: 2590–2599.

[19] Fan X W, Yu S H, Lan H P, Zhang H, Zhang Y C, Liu Y. Study on static pressure damage degree of Korla pear based on electrical properties. Agricultural Mechanization Research, 2021; 9: 194–214. (in Chinese)

[20] Li S Y, Liu Y, Niu X Y, Tang Y R, Lan H P, Zeng Y. Comparison of prediction models for determining the degree of damage to Korla fragrant pears. Agronomy, 2023; 13: 1670.

[21] Guo W C, Shang L, Zhu X H, Nelson S O. Nondestructive detection of soluble solids content of apples from dielectric spectra with ANN and chemometric methods. Food and Bioprocess Technology, 2015; 8: 1126–1138.

[22] Li Y Z, Li C G. The agricultural product wholesale price index forecasting model based on LSSVR optimized by PSO. Journal of Covergence Information Technology, 2012; 7(17): 531–539.

[23] Zhang R, Li S Y, Liu Y, Li G W, Jiang X, Fan X W. Construction of color prediction model for damaged Korla Pears during storage period. Applied Sciences, 2023; 13: 7885.

[24] Komarnicki P, Stopa R, Kuta L, Szyjewicz D. Determination of apple bruise resistance based on the surface pressure and contact area measurements under impact loads. Computers and Electronics in Agriculture, 2017; 142: 155–164.

[25] Yu S H, Liu Y, Tang Y R, Li X L, Li W, Li C, et al. Non-destructive quality assessment method for Korla fragrant pears based on electrical properties and adaptive neural-fuzzy inference system. Computers and Electronics in Agriculture, 2022; 203: 107492.

[26] Wu L, Ogawa Y, Tagawa A. Electrical impedance spectroscopy analysis of eggplant pulp and effects of drying and freezing–thawing treatments on its impedance characteristics. Journal of Food Engineering, 2007; 87(2): 274–280.

[27] Zhu H K, Liu F, Ye Y, Chen L, Liu J Y, Gui A H, et al. Application of machine learning algorithms in quality assurance of fermentation process

of black tea-based on electrical properties. Journal of Food Engineering, 2019; 263: 165–172.

[28] Ma Q, Yang N, Jin Y M, Zhao J J, Jin Z Y, Xu X M. Evaluating quality indices of pickled garlic based on electrical properties. Journal of Food Process Engineering, 2016; 39(1): 88–96.

[29] Seo C, Jo H Y, Byun Y, Ryu J H, Joo Y S. Montmorillonite content prediction in bentonite using Vis–NIR spectroscopy and PLSR analysis: Effects of humidity and mineralogical variability. Geoderma, 2024; 448: 116980.

[30] Zhou L J Y, Wu H B, Jing T T, Li T H, Li J S, Kong L J, et al. Estimation of relative chlorophyll content in lettuce (*Lactuca sativa* L.) leaves under cadmium stress using visible-near-infrared reflectance and machine-learning models. Agronomy, 2024; 14: 427.

[31] Wang X Y, Ling Y, Ling X, Li X H, Li Z C, Hu K P, et al. A particle swarm algorithm optimization-based SVM–KNN algorithm for epileptic EEG recognition. International Journal of Intelligent Systems, 2022; 37: 11233–11249.

[32] Zhang K X, Zuo Z Y, Zhou C A, Chen H, Ding Z T. Research on hyperspectral timely monitoring model of green tea processing quality based on PSO-LSSVR. Journal of Food Composition and Analysis, 2024; 134: 106490.

[33] Li C, Li Z B, Wang X Y, Li W, Lan H P, Liu Y, et al. Using the equivalent static pressure method to assess free fall damage of the Korla fragrant pear. Horticulturae, 2023; 9: 993.

[34] Zhang H, Liu Y, Tang Y R, Lan H P, Niu H, Zhang H. Non-destructive detection of the fruit firmness of Korla fragrant pear based on electrical properties. Int J Agric & Biol Eng, 2022; 15(6): 216–221